



Experimental and theoretical investigation of the mass transfer controlled regime in catalytic monoliths

David H. West^{a,*}, Vemuri Balakotaiah^b, Zoran Jovanovic^c

^a The Dow Chemical Company, 2301 N. Brazosport Boulevard, Freeport, TX 77541-3257, USA

^b Chemical Engineering Department, University of Houston, Houston, TX 77204-4004, USA

^c The Dow Chemical Company, Midland, MI 48674, USA

Abstract

We show that an accurate description of the mass transfer controlled regime in long catalytic monolith channels in which the flow is fully developed and laminar, requires the knowledge of two constants, namely, the asymptotic Sherwood number (Sh_∞ , or dimensionless mass transfer coefficient) and the first normalized Fourier weight, α_1 . While the first of these has received considerable attention in the literature, the second factor has been assumed to be unity. Because of this systematic error (of about 20% for common channel geometries), literature data and correlations for mass transfer in monoliths have large uncertainties. We present new experimental data that corroborates the theory and a new method for experimental estimation of the asymptotic constants for any arbitrary channel shape. For the case of a square channel we obtain experimental values for the constants of $Sh_\infty = 2.92 \pm 0.16$ and $\alpha_1 = 0.78 \pm 0.09$, which are in excellent agreement with the theoretical values ($Sh_\infty = 2.977$ and $\alpha_1 = 0.8074$). Using the asymptotic solutions of the convection–diffusion equation, we develop new correlations for mass transfer coefficients for the case of developing laminar flow that agree with numerical solutions of the Navier–Stokes equations, and theory in the limits.

© 2003 Elsevier B.V. All rights reserved.

Keywords: Mass transfer control; Catalytic monolith; Sherwood number; Mass transfer correlation

1. Introduction

Catalytic monoliths are important for many applications such as automobile emission control, oxidation of volatile organic compounds and power generation. One common form of the monolithic catalytic reactor consists of parallel channels (typically 40–100 cells/cm²) through which the reacting fluid flows. The catalyst is deposited as a thin washcoat layer (10–50 μm thick) on the wall. The flow is laminar in most applications with the Reynolds number in the range 10–1000. As the feed temperature is increased,

the operation of the monolith moves from kinetic to the mass transfer controlled regime. At sufficiently high inlet temperatures, the ignition point moves to the inlet and the entire monolith operates in the mass transfer controlled regime. In this regime, the performance of the monolith depends mainly on the diffusion of reactants transverse to the flow direction. For given physical dimensions of the monolith and flow conditions, the mass transfer controlled regime gives an upper bound on the conversion and hence represents an idealized design for a fixed pressure drop. The goal of this work is to examine the mass transfer controlled regime both theoretically and experimentally. Specifically, we review and extend recent theoretical results and show that the mass transfer controlled

* Corresponding author. Fax: +1-979-238-0651.

E-mail address: dwest@dow.com (D.H. West).

Nomenclature

A_{Ω}	channel cross-sectional area
c	dimensionless reactant concentration
C	reactant concentration
D	channel diameter
D_h	channel hydraulic diameter ($=4R_{\Omega}$)
D_m	molecular diffusivity
f	friction factor
k_c	local mass transfer coefficient
L	length/distance along the monolith channel
P	transverse Peclet number
P_{Ω}	channel perimeter
Re	Reynolds number ($=\langle u \rangle D_h/\nu$)
R_{Ω}	transverse diffusion length ($=A_{\Omega}/P_{\Omega}$)
R_h	channel hydraulic radius ($=2R_{\Omega}$)
Sc	Schmidt number ($=\nu/D_m$)
Sh	Sherwood number ($=4R_{\Omega}k_c/D_m$)
$\langle u \rangle$	average fluid velocity
z	dimensionless axial distance

Greek letters

Γ	gamma function
χ_m	mixing-cup exit conversion
α_1	Fourier weight
μ_1	$=Sh_{\infty}/4$
μ	dynamic viscosity
ν	kinematic viscosity

Subscripts

m	mean/mixing-cup value
0	inlet
∞	asymptotic value

regime in monoliths with long channels ($L/D_h \gg 1$, L = channel length, D_h = hydraulic diameter) is described by two constants that depend on the channel geometry and flow profile. One of these constants is the, well known, asymptotic Sherwood number, Sh_{∞} (dimensionless mass transfer coefficient). [Note: Sh_{∞} is the constant value that the local Sherwood number, $Sh(L)$, approaches as $L/D_h \rightarrow \infty$.] The second constant is the normalized Fourier weight α_1 ($0 < \alpha_1 < 1$), which is usually in the range 0.7–0.9 for fully developed flow in common channel geometries. Most literature correlations (derived from analysis of exper-

imental data) have a systematic error introduced by the assumption $\alpha_1 = 1$. We present new experimental data for square channels and illustrate how the data may be used to obtain experimental estimates of these asymptotic constants. We also use the theory to develop new mass transfer correlations for developing laminar flows.

2. Literature review

Many previous studies of monoliths describing experimental, modeling and simulation results exist in the literature (Wei [1]; Hegedus [2]; Heck et al. [3]; Young and Finlayson [4]; Oh et al. [5]; Hegedus et al. [6]). The recent review articles by Cybulski and Moulijn [7], Lox and Engler [8], Groppi et al. [9] and books by Becker and Pereira [10] and Hayes and Kolaczkowski [11] summarize the progress.

Many correlations exist in the literature for heat and mass transfer in catalytic monoliths. We discuss here only briefly the mass transfer correlations and refer the reader to the recent articles by Gupta and Balakotaiah [12] and Balakotaiah and West [13] for a more detailed review and discussion of the theory and correlations.

The most widely used correlation for estimating mass transfer coefficients in monoliths is that proposed by Hawthorn [14]

$$Sh = Sh_{\infty}[1 + C \times 16P]^{0.45} \quad (1)$$

where Sh_{∞} is the asymptotic Sherwood number attained for the channel and C is a surface roughness constant. {The transverse Peclet number [$P = \langle u \rangle R_{\Omega}^2/(D_m L)$] is related to the Reynolds ($Re = \langle u \rangle D_h/\nu$) and Schmidt numbers (Sc) by $P = (1/16)(D_h/L) Re Sc$, where D_h is the channel hydraulic diameter and L is the distance from the inlet at which the mass transfer coefficient is to be evaluated. The factor 1/16 comes from our definition of R_{Ω} ($= D_h/4$), the transverse diffusion length. This definition of R_{Ω} normalizes the effect of channel shape [13].} The suggested value of C is given by $16C = 0.078$ for smooth surfaces and $16C = 0.095$ for automobile monolith catalysts. Many other correlations also express Sh in terms of Sh_{∞} and P . For example, Holmgren and Andersson [15] fit their data

on gas-solid mass transfer in a square channel with rounded corners (a washcoated monolith) to

$$Sh = 3.53 \exp(0.48P) \quad (2)$$

Both these correlations do not distinguish between fully developed and developing flows at the inlet to the channel. Hence, they do not contain the Schmidt number explicitly but only the transverse Peclet number (i.e., these correlations are independent of the fluid viscosity).

For the case of circular channels, Kirchner and Eigenberger [16] use the correlation

$$Sh = [Sh_1^3 + 0.7^3 + (Sh_2 - 0.7)^3 + Sh_3^3]^{1/3} \quad (3)$$

$$Sh_1 = 3.66 \quad (4)$$

$$Sh_2 = 4.997\sqrt{P} \quad (5)$$

$$Sh_3 = 2 \left(\frac{2}{1 + 22Sc} \right)^{1/6} \sqrt{P} \quad (6)$$

This correlation takes into account the dependence of the Sherwood number on both P and Sc but does not agree with the theoretical results for large values of P (entry region). (Specifically, the values of the exponents on P and Sc in the correlation are different than the theoretical values. There is nothing wrong with this if the goal is simply to fit experimental data for a specific system.) Recently, a correlation based on theoretical results has been presented by Tronconi and Forzatti [17] and Hayes and Kolaczkowski [18], which is given by

$$Sh = Sh_\infty + \gamma_1 P^{\gamma_2} \exp\left(-\frac{\gamma_3}{P}\right) \quad (7)$$

where γ_i ($i = 1, 2, 3$) are numerical constants that depend on the geometry and the Schmidt number. For example, for the case of fully developed flow in a circular channel, the recommended values are $\gamma_1 = 0.914$, $\gamma_2 = 3.575$ and $\gamma_3 = 0.488$ while for the case of developing flow in a circular channel with $Sc = 0.7$, $\gamma_1 = 0.927$, $\gamma_2 = 3.013$ and $\gamma_3 = 0.545$. This correlation takes into account the variation of the Sherwood number with both P and Sc but the constants γ_i have to be fitted for each geometry and Schmidt number.

The mass transfer correlations are combined with the standard one-dimensional two-phase model

$$\langle u \rangle \frac{dC_m}{dz'} = -k_c(z') a_v (C_m - C_s) \quad (8)$$

$$k_c(z') (C_m - C_s) = t_w R_v(C_s) \eta \quad (9)$$

$$C_m = C_0 \text{ at } z' = 0 \quad (10)$$

to predict steady-state conversion in the isothermal case (or the extension of the model with both heat and mass transfer correlations in the non-isothermal case). Here, $\langle u \rangle$ is the average fluid velocity, C_m the cup-mixing concentration of the reactant, C_s the reactant concentration at the solid–fluid interface, η the effectiveness factor, $k_c(z')$ the local mass transfer coefficient, a_v the fluid–solid interfacial area per unit volume, t_w the effective washcoat thickness, and $R_v(C_s)$ the intrinsic reaction rate (based on unit washcoat volume). For the mass transfer limited regime, $C_s = 0$, Eqs. (8) and (10) may be combined and integrated to obtain

$$\ln\left(\frac{1}{1 - \chi_m}\right) = \ln\left(\frac{C_0}{C_{me}}\right) = 4 \int_0^{1/16P} Sh(z^+) dz^+ \quad (11)$$

where χ_m is the exit conversion and the dimensionless axial coordinate z^+ and $Sh(z^+)$ are defined by

$$z^+ = \frac{D_m z'}{16R_\Omega^2 \langle u \rangle} \quad (12)$$

$$Sh(z^+) = \frac{4k_c R_\Omega}{D_m} \quad (13)$$

$$P = \frac{1}{16} \frac{D_h}{L} Re Sc = \frac{1}{4} \frac{R_\Omega}{L} Re Sc \quad (14)$$

Since exit concentration C_{me} (or conversion χ_m) is often measured in the experiments (by changing monolith length or inlet fluid velocity or flow rate), the differential form of Eq. (11) may be used to determine the local Sherwood number, i.e.

$$Sh(P) = \frac{4P^2}{(1 - \chi_m)} \left(-\frac{d\chi_m}{dP} \right) = 4P^2 \frac{d}{dP} [\ln(1 - \chi_m)] \quad (15)$$

It follows from the above review of the classical treatment of the mass transfer limited regime in monoliths, only the Sherwood number (and its dependence on position or P) is needed to predict the exit conversion.

3. Theoretical results for the mass transfer controlled regime

In this section, we review and extend some recent theoretical results for the mass transfer limited regime in catalytic monoliths [13]. We use these results to interpret the experimental data.

We consider a single channel of a monolith of uniform cross-section and assume that the velocity field is unidirectional and does not vary along the channel (this includes the case of fully developed laminar flow; and idealized cases such as flat velocity, and developing laminar flow in the limiting cases of zero or infinite Schmidt number). We assume further that reaction occurs on the wall, or equivalently, that the washcoat is very thin, so diffusional limitations in the washcoat are not important. We also assume that the monolith wall temperature is high enough so that the reaction is infinitely fast and the reactant concentration on the wall is zero. We assume further that the reactant inlet concentration is low enough so that the adiabatic temperature rise is small and the variation of velocity and diffusivity with temperature is negligible. (These two assumptions which may not be satisfied for some data reported in the literature can be relaxed as discussed in the last section.) Finally, we assume that the ratio $L/D_h \gg 1$ (L = channel length, D_h = channel hydraulic diameter) so that the axial diffusion term may be neglected. With these assumptions, the steady-state reactant concentration profile satisfies the following convection–diffusion equation and boundary conditions:

$$\langle u \rangle f(x', y') \frac{\partial C}{\partial z'} = D_m \nabla_*^2 C; \quad 0 < z' < L, \quad (x', y') \in \Omega \quad (16)$$

$$C = C_0; \quad \text{at } z' = 0 \quad (17)$$

$$C = 0; \quad \text{on } \partial\Omega \quad 0 < z' < L \quad (18)$$

Here, Ω denotes the channel cross-section, $\partial\Omega$ is the boundary of Ω , x' and y' are transverse coordinates, ∇_*^2 is the Laplacian in Ω , $\langle u \rangle f(x', y')$ is the local velocity, D_m is the molecular diffusivity of the reacting species, and C_0 is the inlet reactant concentration. Eqs. (16)–(18) contain the following two characteristic times:

$$t_c = \frac{L}{\langle u \rangle}; \quad t_\Omega = \frac{(A_\Omega/P_\Omega)^2}{D_m} = \frac{R_\Omega^2}{D_m} \quad (19)$$

Here, t_c is the convection (or residence) time and t_Ω is the transverse diffusion time. (R_Ω is the effective transverse diffusion length; A_Ω and P_Ω are the cross-sectional area and perimeter of the channel, respectively.) The ratio of these two characteristic times is the *transverse* Peclet number

$$P = \frac{R_\Omega^2 \langle u \rangle}{L D_m} = \frac{t_\Omega}{t_c} \quad (20)$$

Defining

$$\chi = \frac{C_0 - C}{C_0}; \quad z = \frac{z'}{L}; \quad x = \frac{x'}{R_\Omega}; \quad y = \frac{y'}{R_\Omega}; \quad g(x, y) = f(R_\Omega x, R_\Omega y) \quad (21)$$

Eqs. (16)–(18) may be written in the following dimensionless form

$$g(x, y) \frac{\partial \chi}{\partial z} = \frac{1}{P} \nabla^2 \chi; \quad 0 < z < 1; \quad (x, y) \in \Omega \quad (22a)$$

$$\chi = 0 \quad \text{at } z = 0 \quad (22b)$$

$$\chi = 1 \quad \text{on } \partial\Omega \quad (22c)$$

Here ∇^2 is the dimensionless Laplacian operator in the transverse coordinates. With some change of notation, we note that Eqs. (22a)–(22c) define the classical Graetz problem for a duct of uniform cross-section. We also note that z/P is the dimensionless axial distance often used in the heat and mass transfer literature.

The quantity of interest is the mixing-cup or average exit conversion (or dimensionless concentration, $c_m = 1 - \chi_m$) defined by

$$\chi_m = \frac{\int_\Omega g(x, y) \chi(z = 1, x, y) d\Omega}{\int_\Omega g(x, y) d\Omega} \quad (23)$$

It can be seen intuitively that when $P \ll 1$ (transverse diffusion time is much smaller than the convection time) χ_m approaches unity, while for $P \gg 1$, χ_m is small. We can express the general solution of Eqs. (22a)–(22c) in terms of the eigenvalues and eigenfunctions of the Laplacian operator in the domain Ω with weight function $g(x, y)$. Let μ_j ($j = 1, 2, \dots$)

be the j -th eigenvalue and ϕ_j be the corresponding eigenfunction of the self-adjoint eigenvalue problem:

$$\nabla^2 \phi_j = -\mu_j g(x, y) \phi_j \text{ in } \Omega \quad (24)$$

$$\phi_j = 0 \text{ on } \partial\Omega \quad (25)$$

It is easily seen that the eigenvalues are all non-negative ($\mu_j \geq 0$, $j = 1, 2, \dots$) and the eigenfunctions satisfy the orthogonality relation

$$\iint_{A\Omega} \phi_i(x, y) \phi_j(x, y) g(x, y) dx dy = 0, \quad i \neq j \quad (26)$$

Let α_j be the normalized Fourier coefficient defined by

$$\alpha_j = \frac{\langle 1, \phi_j \rangle^2}{\langle 1, \phi_j^2 \rangle} \quad (27)$$

where the inner product in Eq. (27) is defined by

$$\langle \phi_i, \phi_j \rangle = \frac{\iint_{A\Omega} \phi_i(x, y) \phi_j(x, y) g(x, y) dx dy}{\iint_{A\Omega} g(x, y) dx dy} \quad (28)$$

[It follows from Parseval's theorem that the constants α_j sum to unity.] The exit mixing-cup concentration or conversion is given by

$$c_m = 1 - \chi_m = \sum_{j=1}^{\infty} \alpha_j \exp\left(-\frac{\mu_j}{P}\right) \quad (29)$$

We can also calculate the local Sherwood number as a function of P (axial position) from the above relationship between χ_m and P and Eq. (15). Substitution of Eq. (29) in Eq. (15) gives

$$Sh(P) = 4 \frac{\sum_{i=1}^{\infty} \alpha_i \mu_i \exp(-(\mu_i/P))}{\sum_{i=1}^{\infty} \alpha_i \exp(-(\mu_i/P))} \quad (30)$$

Thus, the same constants α_i and μ_i ($i = 1, 2, \dots$) determine the Sherwood number or the local mass transfer coefficient as a function of axial distance (P). It should be noted that Eq. (30) is valid for any arbitrary channel geometry but only for the case of unidirectional velocity profile. We give in Table 1 the first few constants α_i and μ_i for circular and square channels for the case of fully developed laminar flow ($Sc = \infty$). A more extensive list for other geometries is given in Balakotaiah and West [13].

We now consider various limiting cases.

Table 1

The first four constants α_j and μ_j for fully developed laminar flow in square and circular channels

j	Square		Circle	
	α_j	μ_j	α_j	μ_j
1	0.8074	0.7443	0.8190	0.9142
2	0.1041	4.432	0.0975	5.576
3	0.0133	9.821	0.0325	14.24
4	0.0351	13.473	0.0154	26.91

3.1. Fully developed laminar flow

For fully developed laminar flow and P values of order unity or smaller (the practical case of long channels), the conversion (or concentration) may be approximated by Eq. (29) by using only the first term. Thus, we have

$$1 - \chi_m \approx \alpha_1 \exp\left(-\frac{\mu_1}{P}\right), \quad \text{for } P < 1 \quad (31)$$

Similarly, for $P < 1$, the Sherwood number given by Eq. (30) may be approximated by the asymptotic value

$$Sh_{\infty} = 4\mu_1 \quad (32)$$

This one term truncation (Eq. (31)) of the exact solution (which gives three decimal place accuracy for $P < 1$) should be compared with the solution of the standard two-phase model (Eqs. (8)–(10)). Under the assumption of constant k_c and mass transfer control ($c_s = 0$), Eqs. (8) and (10) may be integrated to obtain

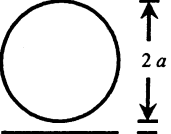
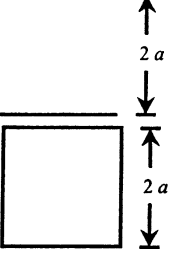
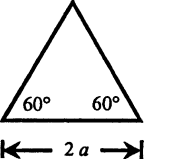

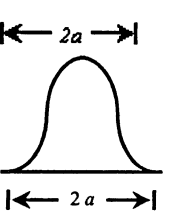
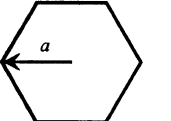
$$1 - \chi_m = \exp\left(\frac{-Sh_{\infty}}{4P}\right) = \exp\left(\frac{-\mu_1}{P}\right)$$

This equation differs from the correct solution (Eq. (31)) by the factor α_1 . As can be seen from Table 2, this widely used approximation introduces a systematic error of as much as 20% in the computed exit concentration for square channels (and the error may be of similar magnitude for other geometries). This systematic error is one reason for the disagreement between various mass transfer correlations reported in the literature.

For $P \gg 1$ (which correspond to the entry region), it may be shown [13] that the asymptotic form of Eq. (29) is

$$\chi_m = \frac{\beta_{\infty}}{P^{2/3}} \quad (P \gg 1) \quad (33)$$

Table 2
Effective diffusion length, asymptotic constants, and friction factor for some common channel shapes

Channel shape	$R_h = 2R_\Omega$	Sh_∞	$f Re$	α_1
	a	3.656	16	0.81905
	$2a$	7.541	24	0.91035
	$\frac{a}{\sqrt{3}}$	2.496	13.33	0.7753
	$\frac{2a}{3}$	3.392	15.548	0.7891
	$0.770a$	2.966	14.65	0.7872
	$\frac{\sqrt{3}}{2}a$	3.34	15.05	0.8156

$$\beta_\infty = \frac{3^{4/3}(f Re)^{1/3}}{4\Gamma(1/3)} = 0.404(f Re)^{1/3} \quad (34)$$

where f is the friction factor and $Re = D_h \langle u \rangle / \nu$ is the duct Reynolds number. Similarly, for $P \gg 1$, the asymptotic form of the expression for the Sherwood number is given by

$$Sh(P) = \frac{8}{3}\beta_\infty P^{1/3} = 1.077(f Re)^{1/3} P^{1/3} \quad (P \gg 1) \quad (35)$$

This relation shows that the entry region mass transfer correlations should be consistent with the friction factor data for the duct.

In the literature, the exact expression for the Sherwood number given by Eq. (30) is often replaced by simplified expressions. One such expression is obtained by simply adding the entry region and downstream asymptotes:

$$Sh(P) = Sh_\infty + 1.077(f Re)^{1/3} P^{1/3} \quad (36)$$

While this expression has little error in the limits of $P \rightarrow 0$ (asymptotic region) and $P \rightarrow \infty$ (entry region), it has considerable error for P values of order unity (e.g. in the corner region where the two asymptotes meet, the above expression overpredicts the Sh value by as much as 50%). The error can be reduced by using the asymptotes separately, i.e.

$$Sh = \begin{cases} 1.077(f Re)^{1/3} P^{1/3} & \text{for } P > \frac{0.8Sh_\infty^3}{f Re} \\ Sh_\infty & \text{for } P \leq \frac{0.8Sh_\infty^3}{f Re} \end{cases} \quad (37)$$

Empirical correlations similar to Eq. (36) but having smaller error can also be developed for any specific geometry by matching the asymptotes and the Sherwood number at intermediate values with that given by the exact expression. One appealing feature of Eq. (37) is that it is valid for any arbitrary geometry and requires knowledge of only one additional asymptotic constant (Sh_∞) if the friction factor relationship is known for the duct. Table 2 gives the asymptotic Sherwood number, friction factor, and α_1 for some common channel shapes.

We show in Fig. 1 a plot of the exact expression for the Sherwood number for fully developed laminar flow in a circular channel (solid line) and compare it with the approximate correlation given by Eq. (37) (dotted line). As expected, the approximate correlation obtained by patching together the large and small P asymptotes approximates the exact Sherwood number with reasonable accuracy. The maximum relative error is at the corner where the two asymptotes meet. At this point, Eq. (37) underpredicts the mass transfer coefficient by about 10%. This accuracy may be sufficient for many applications.

3.2. Developing laminar flow

We now consider the case of developing laminar flow. For this case, the conversion and the Sherwood number depend on the Schmidt number and the exact values can be obtained only by solving the Navier–Stokes equations along with the convection–diffusion equation. However, the two limiting cases of $Sc = 0$ and $Sc = \infty$ can be analyzed using the theory presented above. The case $Sc = 0$ which corresponds to the case of flat velocity ($g(x, y) = 1$) is of

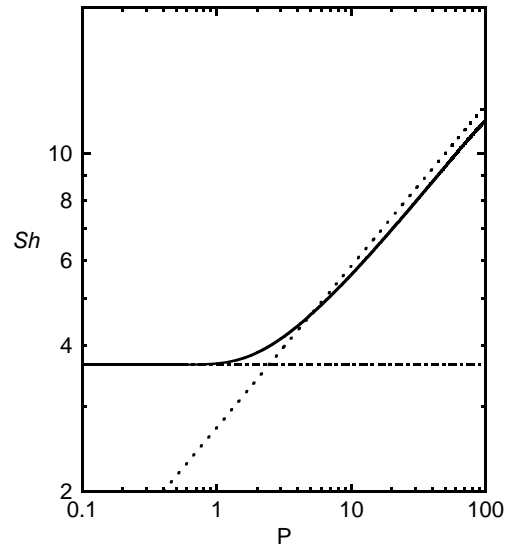


Fig. 1. Dependence of the Sherwood number on the transverse Peclet number for a circular channel. The analytical expression (Eq.(30), solid line) is compared with the small- P (dash-dot line) and large- P (dashed line) asymptotes (Eq. (37)).

special interest since it gives an upper bound on χ_m and Sh for any given P (provided turbulence effects can be neglected at the entrance to the channel). The constants α_i and μ_i ($i = 1, 2, \dots$) can be determined analytically for the case of flat velocity profile for some common duct geometries. For example, for the case of a circular duct,

$$\alpha_j = \frac{1}{\mu_j} = \frac{\lambda_j^2}{4} \quad (38)$$

where λ_j is the j -th zero of the Bessel function $J_0(\lambda)$. When $g(x, y) = 1$, it is easily seen that the two asymptotes of Eq. (30) are given by

$$Sh = \begin{cases} \frac{4}{\sqrt{\pi}} P^{1/2} & \text{for } P \rightarrow \infty \\ 4\mu_1 & \text{for } P \rightarrow 0 \end{cases} \quad (39)$$

We note that the large P asymptote is independent of the geometric shape of the channel while the small P asymptote (which is equal to four times the first eigenvalue of the Laplacian operator in Ω with Dirichlet boundary condition on $\partial\Omega$ and with $g(x, y) = 1$) varies with the geometry of the channel. Similarly, for $P \gg 1$ the conversion is indepen-

dent of the channel geometric shape and is given by $\chi_m = 2/\sqrt{\pi P}$.

We now consider the case of developing flow with finite Schmidt number. We have already seen that the conversion is nearly unity and independent of Sc in the limit $P \rightarrow 0$. However, it is more appropriate to compare the exit concentration rather than conversion in the limit $P \rightarrow 0$. For P values of order unity or smaller, the concentration for the limiting cases of $Sc = 0$ and $Sc = \infty$ may be approximated by Eq. (31). Though the solution of the convection–diffusion equation for the case of developing flow is not in the form given by Eq. (31), the variation in the values of these constants α_1 and μ_1 is indicative of the influence of the Schmidt number on conversion and the asymptotic Sherwood number for the case of $P < 1$. Examination of the numerical values in Table 1

$$Sh(L) = \begin{cases} 1.4P^{1/2}Sc^{-1/6} = 0.35 \left(\frac{D_h}{L}\right)^{1/2} Re^{1/2} Sc^{1/3} & \text{for } P > 0.51Sh_\infty^2 Sc^{1/3} \\ Sh_\infty & \text{for } P < 0.51Sh_\infty^2 Sc^{1/3} \end{cases} \quad (41)$$

shows that the constant α_1 increases by about 25% as Sc increases from zero to infinity. The asymptotic Sherwood number ($= 4\mu_1$) which is more important in practice (as it appears in the exponent), decreases as much as 50% as the Schmidt number increases from zero to infinity. Not accounting for this variation of the Sherwood number on Sc is a second source of systematic error in some published correlations for mass transfer in monoliths.

For any finite Schmidt number, the Sherwood number approaches the asymptotic Sherwood number (Sh_∞) for the fully developed case ($Sc = \infty$) as $P \rightarrow 0$. For $P \gg 1$ and finite Sc , it may be shown that [13]

$$Sh = \frac{1.4\sqrt{P}}{Sc^{1/6}}; \quad P \gg 1 \quad (40)$$

Thus, the curve Sh versus P for any finite Schmidt number is parallel to the curve corresponding to the flat velocity profile ($Sc = 0$) case for $P \gg 1$ and approaches the fully developed curve for $P \ll 1$. As observed earlier, the large P behavior for any finite Schmidt number is independent of the geometric shape. Thus, Eq. (40) is valid (in the limit of large P) for developing flow in a channel of

arbitrary shape. Unfortunately, this asymptote is approached very slowly, so Eq. (40) only gives accurate estimates of Sherwood number for P values greater than about 100. We address this in the next section.

3.3. Mass transfer correlations for developing laminar flows

It follows from the above discussion that the Sherwood number for the case of developing flow must approach that corresponding to the fully developed case for $P \rightarrow 0$ while in the entry region it is independent of the duct geometric shape and is given by Eq. (40). A simple approximation for Sh valid for any arbitrary geometry may be obtained by simply combining the small and large P asymptotes:

As in the case of fully developed flow, this equation is accurate for large and small P values. The error in this correlation can not be determined (because we do not have the exact solution for the simultaneously developing flow case) but based on the fully developed case, we expect the error to be about 10% when $Sc > 5$ (underpredicting the Sherwood number) in the transitional (corner) region between the asymptotes. It is applicable to developing flow in any arbitrary geometry and requires only knowledge of the fully developed asymptotic Sherwood number. The second term of this expression is the asymptotic Sherwood number corresponding to fully developed flow and concentration fields, while the first term corresponds to a developing concentration field in a fully developed flow field. (It is the Pohlhausen solution for mass transfer in a laminar boundary layer.)

A comparison of Eq. (41) with the numerical data for circular channel given by Shah and London [19] for $Sc = 0.7$ (air) shows that the correlation is accurate for small and large P values (as expected) but may underestimate the Sherwood number by as much as 50% near the transition. (In contrast, the maximum error for the fully developed case is around 10%.) This error can be reduced by using an empirical expression

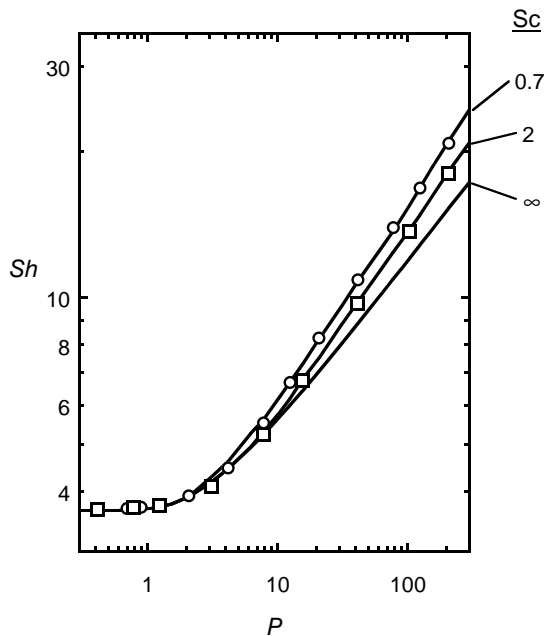


Fig. 2. Comparison of Sh derived from numerical solutions of the Navier–Stokes equations (by Shah and London [19]; lines) with our correlation (Eq. (42)) for $Sc = 0.7$ (circles) and $Sc = 2$ (squares).

of the form

$$Sh = Sh_{\infty} + \frac{1.4 a Sc^{-1/6} P^2}{1 + b P^{3/2}} \quad (42)$$

and fitting the values of a and b . For the case of a circular channel with $Sc = 0.7$, we obtain $a = 0.0469$, $b = 0.0584$. It is found that the same constants also describe the data for $Sc = 2$. Fig. 2 compares Sh derived from numerical solutions of the Navier–Stokes equations by Shah and London [19] (solid lines) with the correlation above (Eq. (42), symbols). The maximum error in the correlation is about 3%. We note that for $Sc \geq 5$ and the practical range of P values ($0 < P < 100$), the Sherwood number for the developing flow case is nearly identical to that of the fully developed case (line corresponding to $Sc = \infty$). Thus, Eq. (42) is recommended for estimating Sh for Sc values close to unity. Since the effect of channel geometry appears only through the first term, we expect Eq. (42) to be valid for other channel geometries and Sc numbers around unity. However, we have no

data to verify the accuracy of this correlation for other geometries.

4. Comparison of theory with data from the literature

In this section, we compare our theoretical results with some selected data from the literature. As shown above, when the flow is laminar, the solutions of the convection diffusion equation for the cases of $Sc = 0$ and $Sc = \infty$ give the upper and lower bounds, respectively, on conversion in the mass transfer controlled regime. (The solution for $Sc = \infty$ is a lower bound for the mass transfer controlled regime in the sense that no data should fall below this line unless there is significant kinetic or diffusional limitations (within the washcoat).) Since we have an expression for the conversion we can use conversion data directly (eliminating the propagation of error inherently introduced when differentiating conversion to compute the Sherwood number).

Fig. 3 compares data from two previous works (with square channels) with these bounds. The data

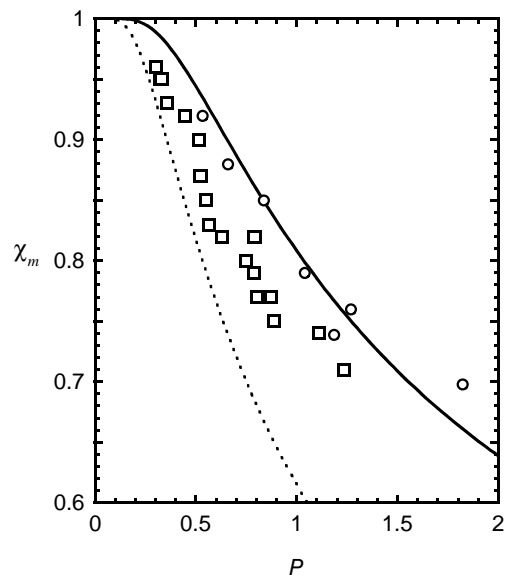


Fig. 3. Exit conversion vs. transverse Péclet number for square channels. Experimental data of Uberoi and Pereira [20] (circles) and Holmgren and Andersson [15] (squares) are compared with the theoretical upper ($Sc = 0$, solid line) and lower ($Sc = \infty$, dashed line) bounds.

of Uberoi and Pereira [20] lies close to the line corresponding to a flat velocity profile ($Sc = 0$), but one point is slightly above the line. It is possible to exceed the upper bound if there is still turbulence in the flow or if there is a large adiabatic temperature rise. The latter explanation can be ruled out in the case of Uberoi and Pereira's work, because they used low CO concentrations (200 ppm). The data of Holmgren and Andersson [15] lies between the two theoretical limits; their results are closer to the lower bound ($Sc = \infty$) for experiments with small values of P (about 0.5) and closer to the upper limit ($Sc = 0$) for the data point with the highest value of P (about 1.3). Conversion data in excess of that expected for fully developed flow can be caused by flow development or turbulence within the channels as discussed by Holmgren and Andersson [15]; they observed the same trend when comparing their results with numerical simulations (which included turbulent diffusion). The fraction of the channel length in which the velocity profile is still developing is smaller in experiments with low values of transverse Peclet number (larger L/D or lower velocity). In short monoliths (relatively small L/D) more of the channel length is required to develop the velocity profile.

Recently, Khinast et al. [21] did experiments in a circular tube in which the entry section was not catalyzed to allow the flow to develop and turbulence to dissipate prior to entering the catalyzed section of the tube. Fig. 4 compares their data for the case of 1% CO with the solutions for $Sc = 0$ and $Sc = \infty$. Their data lie above the line corresponding to fully developed flow, like in the previously discussed work with square channels. In their experimental apparatus, a thermocouple was placed transverse to the flow just upstream from the reactor inlet. Perhaps vortices in the wake of this thermocouple are responsible for transport rates in excess of that expected for developed laminar flow. For a given residence time (or P) the importance of turbulent transport should increase with tube diameter.

The scaling of the turbulence dissipation rate with channel diameter deserves further comment. The time scale for dissipation of turbulence goes like $t_d \sim \rho D_i^2 / \mu_t$ (where μ_t is the turbulent viscosity, and D_i is the difference in length between the integral scale (channel hydraulic radius) and the Kolmogorov

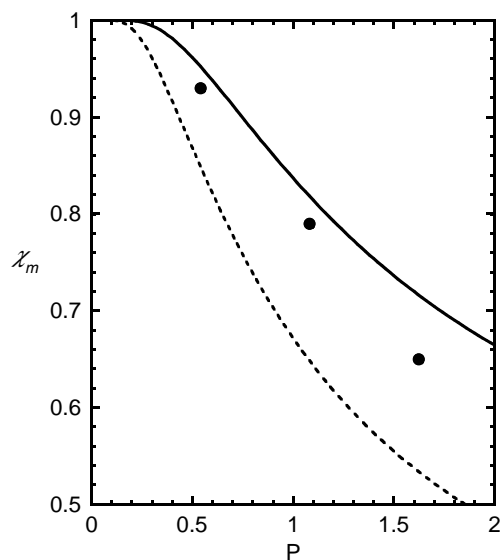


Fig. 4. Exit conversion vs. transverse Peclet number for circular channels. Experimental data of Khinast et al. [21] (symbols) are compared with the theoretical upper ($Sc = 0$, solid line) and lower ($Sc = \infty$, dashed line) bounds.

scale). Tube diameters used in the three previous works compared here are 9.35 mm (Khinast et al. [21]), 3.45 mm and 6.05 mm (Uberoi and Pereira [20]), and 2.09–2.22 mm (Holmgren and Andersson [15]). Since the turbulence dissipation time scale varies quadratically with the channel diameter (while the duct Reynolds number varies linearly and corresponds to eventual laminar flow conditions), even at equal Reynolds numbers, turbulence effects are smaller in small diameter channels than large diameter channels and become negligible as the channel diameter approaches the Kolmogorov scale. We conclude from these scaling arguments that the small channel diameter used in our experiments was adequate for dissipating the turbulence, while the deviation from theory observed in the results of Holmgren and Andersson [15], Uberoi and Pereira [20], and Khinast et al. [21] is likely due to the effect of velocity profile development or turbulence within the monolith channels. For example, if the turbulent viscosity is 10 times the kinematic viscosity, then the time required to dissipate turbulence under the conditions used in ref. [21] is approximately 0.25 s, which is of the same order as the residence time (0.35 s).

5. Experimental results

Two types of monoliths were used: one made of acicular mullite with 64 square channels, 0.132 cm channel diameter, 7.5 cm long; and another made of cordierite with 81 channels, 0.114 cm channel diameter, 7.5 cm long. Both monoliths were square in cross section, approximately 1.3 cm on a side. The monoliths were catalyzed by dipping the blank monolith into a dilute ammonia solution of diamminedinitroplatinum, 1.7%, repeatedly until a Pt loading of 14.4 g/l was obtained. The monoliths were then heated to 200 °C to decompose the platinum salt to platinum oxide, which was then reduced at 225 °C in 5% hydrogen. A washcoated acicular mullite monolith was prepared by the method of incipient wetness using an aqueous alumina slurry, 20%, having a particle size of 120 nm and a surface area after firing of 155 m²/g. After firing, the coated monolith had surface area of 3×10^4 m²/l. Platinum was deposited as described above to give a loading of 2.1 g/l. The catalyzed monolith was fastened into a square 2.54 cm i.d. stainless steel sample holder using InteramTM Mount Mat (3M Corporation). Air, N₂, and CO gas flows were measured using calibrated (Brooks) mass flow controllers. The gasses were mixed in a manifold then preheated by flowing over a nichrome wire prior to entering the reactor section. The oxygen concentration was held constant at 3.2% by volume, while CO was varied in the range 0.1–1.0%; the balance was nitrogen. The total flow rate was varied in the range 40–60 standard l/min, giving Reynolds numbers between 170 and 390. The temperature of the gas entering the monolith was measured by a type K thermocouple located in the sample holder approximately 4.5 cm upstream from the front face of the monolith. Composition of the gas mixture exiting the sample holder was continuously monitored using CO, O₂, and CO₂ analyzers (Servomex 1440 series, or California Analytical Instruments 300). Inlet and outlet CO concentrations were recorded after gas and sample temperatures reached steady-state, and the corresponding CO conversion was calculated as an average of several experiments. Physical properties of the gas were calculated based on the arithmetic mean of the inlet and outlet gas temperatures. In a typical experiment, the feeds were mixed and heated to the same temperature as the catalyst prior to entering the catalyst test section. We

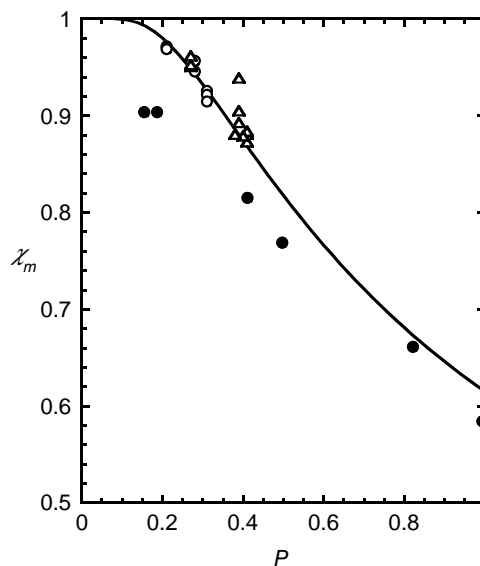


Fig. 5. Exit conversion vs. transverse Peclet number for square channels. The theoretical solution for fully developed flow ($Sc = \infty$, line) is compared with experimental data for non-washcoated acicular mullite (open circles) and cordierite (triangles) monoliths, and a washcoated acicular mullite monolith (solid circles).

confirmed operation in the mass transfer controlled regime by measuring exit conversion at increasingly higher temperatures, until the conversion was found to be independent of temperature. Depending on the flow rate, temperatures in the range 530–700 K were sufficient to establish mass transfer control.

Fig. 5 is a plot of exit conversion versus transverse Peclet number for three different monoliths. The theoretical line for fully developed flow is also shown. We chose flow conditions such that $P < 1$ to minimize the effect of flow development. The exit conversion for both of the non-washcoated monoliths (acicular mullite (open circles) and cordierite (open triangles)) is very close to the theoretical line. We obtained lower conversion with the washcoated acicular mullite monolith (solid circles), apparently because of diffusion limitations within the washcoat. For $P < 1$, a plot of $\ln(1 - \chi_m)$ versus $1/P$ should give a straight line with slope equal to μ_1 and y-intercept equal to $\ln \alpha_1$ (see Fig. 6). From linear regression of the data shown in Fig. 6 we obtain $\mu_1 = 0.73 \pm 0.04$ and $\alpha_1 = 0.78 \pm 0.09$ (where the uncertainty in the parameters

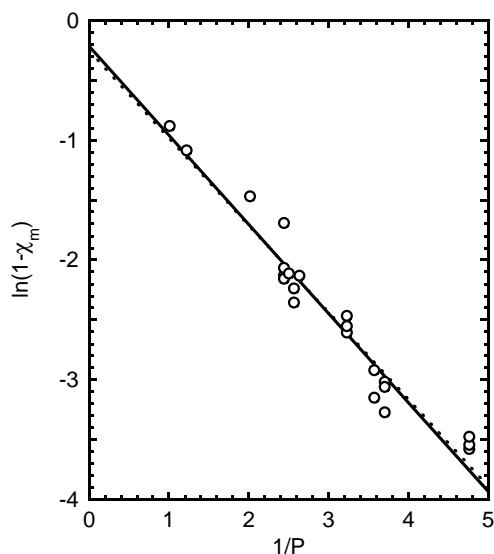


Fig. 6. Plot of $\ln(1 - \chi_m)$ vs. $1/P$ used to determine experimental values for α_1 and μ_1 . Experimental data (circles) and regression fit (dashed line) are compared with the theoretical line for fully developed flow (solid line).

is the standard error of the estimate). These numbers are in excellent agreement with the theoretical values for a square channel ($\mu_1 = 0.7443$, $\alpha_1 = 0.8074$). (In the figure, the best fit line is almost indistinguishable from the theoretical line.) This method can be used to estimate μ_1 and α_1 for other channel geometries for which theoretical values are not known, so it is unnecessary to simply assume $\alpha_1 = 1$.

A systematic error may be introduced by flow variations in the radial direction caused by the shape of the turbulent velocity profile upstream from the monolith. In our experiments the monoliths were centered inside the sample holder such that the upstream face of the monolith was exposed to the middle half of the flow. For the flow conditions of our experiments we expect as much as 10% variation in flow rate from the outermost channels to the center. This variation would tend to decrease the average conversion and could cause data to fall below the theoretical line corresponding to fully developed flow, even if the flow is fully developed within each channel. In order to check for flow variations in the radial direction we did the following experiments. A circumferential notch was cut through the outside walls (2.54 cm from the inlet) of a monolith

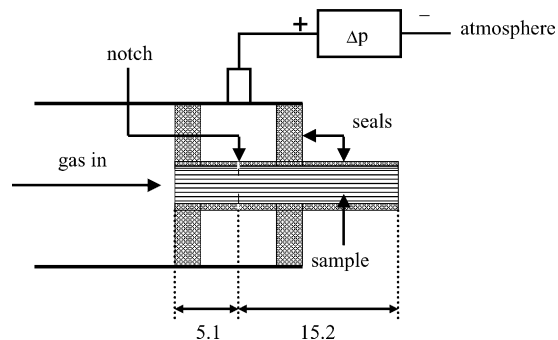


Fig. 7. Experimental apparatus for pressure drop measurements. All dimensions are in cm.

(1.3 cm on a side, 8 cm long) exposing the outermost row of channels. The monolith was then fixed in a square tube (5.1 cm i.d.) with rubber seals as shown in Fig. 7. We measured the pressure difference between the notched test section and the exit as a function of (nitrogen) flow rate. (The purpose of the notch was to allow for velocity profile development.) The monolith was removed and the notch cut further exposing the two outermost rows of channels, and the experiment

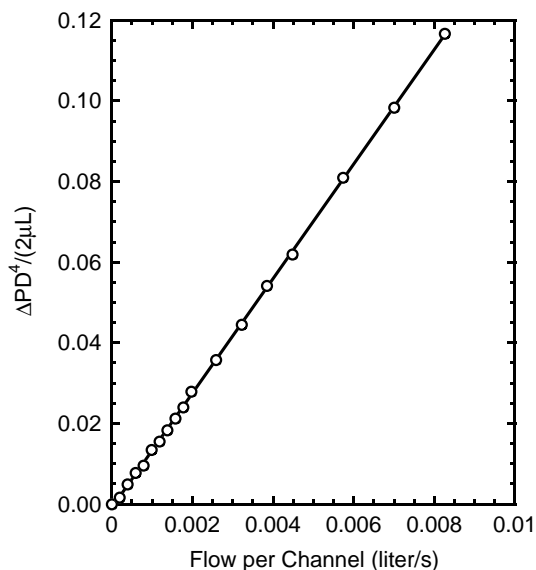


Fig. 8. Plot of $\Delta PD^4 / (2\mu L)$ vs. volumetric flow rate per channel (l/s); experimental data (symbols) and the regression fit of the data (line) are shown.

was repeated. Finally, it was repeated again with the notch cut deeper still to expose the outer three rows of channels. The same results were obtained in all three experiments indicating there was no measurable flow variation in the radial direction. Likewise, similar results were obtained with a cordierite monolith. Fig. 8 shows a plot of $\Delta PD^4/(2\mu L)$ versus volumetric flow rate per channel, for the experiment with a notch exposing the outer two rows of channels. From the slope of the best fit line through the data we obtain the friction factor, $f Re = 14.19 \pm 0.05$, which agrees with the theoretical value (14.2). Thus, we conclude that the flow was nearly uniformly distributed in our experiments.

6. Conclusions and discussion

We have shown that experimental conversion data taken in the mass transfer controlled regime can be used directly to determine the asymptotic constants (namely the Sherwood number, $Sh_\infty = 4\mu_1$ and the Fourier weight α_1) for any channel shape; they are given by the slope and intercept (respectively) of a plot of $\ln(1 - \chi_m)$ versus $1/P$. Using this approach we obtained experimental values for the asymptotic Sherwood number of 2.92 ± 0.16 and normalized Fourier weight ($\alpha_1 = 0.78 \pm 0.09$) for square channels which agree with the theoretical values ($Sh_\infty = 2.977$, $\alpha_1 = 0.8074$) within experimental error. It is clear from the comparisons of data and theory presented here that the effects of flow development and turbulence should be minimized in experiments if the results are to be compared with theory or used in a more general way. The flow development effect can be minimized by taking data in the region of small transverse Peclet number ($P < 1$); this also simplifies the analysis considerably. The time scale for turbulence dissipation is proportional to the square of the channel diameter, so turbulence effects can be minimized by using monoliths with small channel diameter. We estimate the Kolmogorov length scale to be on the order of 0.05 cm for the conditions of our experiments which is roughly one half the channel diameter. Our experimental data for conversion (and Sherwood number) agree well with the theoretical values for fully developed flow. We attribute this good agreement to the small channel diameter (~ 0.1 cm), small CO concentrations ($< 1\%$),

and small values of transverse Peclet number ($P < 1$) used in our experiments.

A systematic error may be introduced by flow variation in the radial direction caused by the shape of the turbulent velocity profile upstream from the monolith. We minimized flow maldistribution in our experiments by centering the monolith within the center half of the flow and sealing the annulus with insulation. The effectiveness of this approach was verified with pressure drop measurements in the outer channels.

New mass transfer correlations derived from theory are presented (given by Eqs. (37) and (41)) for fully developed, as well as developing laminar flows, for channels of arbitrary shape. These correlations are more general compared to prior literature correlations and require knowledge of only the friction factor and the asymptotic Sherwood number for the specific channel shape. In the case of fully developed flow, and for developing flows with $Sc \geq 5$, these correlations have a maximum error of about 10%. For the special case of developing flow with Schmidt number close to unity (which is of practical interest), we have developed a new correlation for circular channels (Eq. (42)) that has a maximum error of about 3%. We conjecture that this correlation should be valid for other geometries as well, but currently lack the data needed to test this assertion. The new correlations that we have presented in this paper correctly reduce to the theoretical values in the limits of small and large P .

An important effect not considered in this work is the influence of physical property variations on the exit conversion in the mass transfer controlled regime. Even when the entire monolith is in the mass transfer controlled regime, the gas velocity and reactant species diffusivity can vary with position due to variation of the gas temperature. This variation can be neglected only when the inlet temperature (T_0) is high and the adiabatic temperature rise (ΔT_{ad}) is small, or equivalently, the ratio $\beta = (\Delta T_{ad}/T_0) < 0.01$. If this is not the case, a correction to the predicted conversion should be made in interpreting the experimental data. Assuming an adiabatic channel, we can use the approximations

$$\frac{\langle u \rangle}{\langle u \rangle_0} = \frac{T}{T_0} = 1 + \beta\chi \quad (43)$$

$$\frac{D_m}{D_{m0}} = \left(\frac{T}{T_0} \right)^\delta = (1 + \beta\chi)^\delta \quad (44)$$

where χ is the local conversion and the constant δ is approximately 1.75 for most gases. Neglecting the pressure drop, the variation of the dimensionless concentration $c_m (= 1 - \chi)$ along the channel is now given by

$$\frac{dc_m}{dz} = -\frac{Sh(z)}{4P} c_m [1 + \beta(1 - c_m)]^{\delta-1} \quad (45)$$

$$c_m(z = 0) = \alpha_1 \quad (46)$$

where $Sh(z)$ is given by Eq. (30) with P replaced by P/z . When $\beta = 0$ and $P < 1$, physical property variation is negligible and integration of the above equations leads to the one term expression given by Eq. (31). For $\beta > 0$, the above equations may be integrated numerically to determine the exit conversion as a function of the transverse Peclet number. We note that the resulting conversion is slightly higher than that predicted by assuming constant physical properties. This correction was found to be negligible in all the experimental data analyzed here except that of Khinast et al. [21], where the correction is small (in the order of 1–2% conversion). The correction factor may be included in P if the diffusivity and velocity are evaluated at the average temperature rather than at the inlet temperature. This can also be seen from Eq. (45). When $\beta < 0.1$, the second factor is close to unity and can be replaced by its average value and included as a correction to P , which is equivalent to evaluating P at the average properties. However, this procedure is no longer valid (and the correction due to physical property variation is substantial) when $\beta > 1$.

Acknowledgements

The work of V. B. was supported by grants from the Robert A. Welch foundation, Texas Advanced Technology Program and The Dow Chemical Company. We thank Mrs. Janet Goss and Dr. Sten Wallin for making the acicular mullite monoliths, and Dr. Greg

Rickle for catalyzing the monoliths used in this work. Finally, we thank an anonymous reviewer for suggesting that flow maldistribution could be important.

References

- [1] J. Wei, The catalytic muffler, *Am. Chem. Soc.* 148 (1975) 1–25.
- [2] L.L. Hegedus, *AIChE J.* 22 (1976) 477–484.
- [3] R.H. Heck, J. Wei, J.R. Katzer, *AIChE J.* 21 (1975) 849–853.
- [4] L.C. Young, B.A. Finlayson, *AIChE J.* 22 (1976) 331–353.
- [5] S.H. Oh, K. Baron, J.C. Cavendish, L.L. Hegedus, *ACS Symp. Ser.* 65 (1978) 461–474.
- [6] L.L. Hegedus, S.H. Oh, K. Baron, *AIChE J.* 23 (1977) 632–642.
- [7] A. Cybulski, Moulijn, *Monoliths in heterogeneous catalysis*, *Catal. Rev. Sci. Eng.* 36 (1994) 179–270.
- [8] E.S.J. Lox, B.H. Engler, in: G. Ertl, J. Weitkamp, H. Knozinger (Eds.), *Handbook of Heterogeneous Catalysis*, Vol. 4, Wiley, New York, 1997, pp. 1559–1633.
- [9] G. Groppi, E. Tronconi, P. Forzatti, *Mathematical models of catalytic combustors*, *Catal. Rev. Sci. Eng.* 41 (1999) 227–254.
- [10] E.G. Becker, C.J. Pereira (Eds.), *Computer Aided Design of Catalysts*, Marcel Dekker, New York, 1993.
- [11] R.E. Hayes, S.T. Kolaczkowski, *Introduction to Catalytic Combustion*, Gordon and Breach, The Netherlands, 1997.
- [12] N. Gupta, V. Balakotaiah, *Chem. Eng. Sci.* 56 (2001) 4771–4786.
- [13] V. Balakotaiah, D.H. West, *Chem. Eng. Sci.* 57 (2002) 1269–1286.
- [14] R.D. Hawthorn, *AIChE Symp. Ser.* 70 (137) (1974) 428–438.
- [15] A. Holmgren, B. Andersson, *Chem. Eng. Sci.* 53 (1998) 2285–2298.
- [16] T. Kirchner, G. Eigenberger, *Chem. Eng. Sci.* 51 (1996) 2409–2418.
- [17] E. Tronconi, P. Forzatti, *AIChE J.* 38 (1992) 201–210.
- [18] R.E. Hayes, S.T. Kolaczkowski, *Chem. Eng. Sci.* 49 (1994) 3587–3599.
- [19] R.K. Shah, A.L. London, *Laminar Flow Forced Convection in Ducts*, *Advances in Heat Transfer*, supplement 1, Academic Press, New York, 1978.
- [20] M. Uberoi, C.J. Pereira, *Ind. Eng. Chem. Res.* 35 (1996) 113–116.
- [21] J.G. Khinast, A. Bauer, D. Bolz, A. Panarello, *Chem. Eng. Sci.* 58 (2003) 1063–1070.